Convection of Paramagnetic Fluid in a Cube Heated and Cooled from Side Walls and Placed below a Superconducting Magnet*
- Comparison between Experiment and Numerical Computations-

Tomasz BEDNARZ [†,‡], Elzbieta FORNALIK [§], Toshio TAGAWA [#], Hiroyuki OZOE [‡]
and Janusz S. SZMYD [§]

Abstract

The magnetic convection of paramagnetic fluid is studied in a strong magnetic field. The fluid in a cubic enclosure is heated from one vertical wall and cooled from the opposite one. The fluid is the 80% mass aqueous solution of glycerol with 0.8 mol/kg concentration of gadolinium nitrate hexahydrate to make the working fluid paramagnetic. The small amount of liquid crystal slurry is added to the fluid in order to visualize the temperature profiles in a vertical cross-section. This system is placed directly below the solenoid of the superconducting magnet which is oriented vertically. The temperature of cold wall is constantly controlled by the water flowing from a thermostating bath. On the other hand, the hot wall is heated by a nichrome wire from a DC power supply. In the numerical computations, the configuration of the system is modeled to be as close as possible to the real system. The physical properties of the working fluid are used to compute dimensionless parameters in the numerical model and the computations are carried out for corresponding cases. Later, the numerical and experimental results are compared with each other.

Key Words: *Magnetic convection, Cubic enclosure, Numerical analysis, Visualization, Particle Image Thermometry*

Nomenclature

b	:	magnetic induction	[T]
b_0	:	$(=\mu_m i/l)$ reference magnetic induction	[T]
B	:	$(= b/b_0)$ dimensionless magnetic induction	[-]
C	:	$(= 1+ 1/(\beta\theta_0))$ dimensionless momentum parameter for paramagnetic fluid	[-]
e_z	:	unit vector in the vertical direction	[-]
g	:	gravitational acceleration	[m/s^2]
i	:	electric current in a coil	[A]
l	:	length of the cubic enclosure	[m]
Nu	:	$(= Q_{cv}/Q_{cd})$ Nusselt number	[-]
p	:	pressure	[Pa]
p_0	:	$(= \rho_0\alpha^2/l^2)$ reference pressure	[Pa]
P	:	$(= p/p_0)$ dimensionless pressure	[-]
Pr	:	$(= \nu/\alpha)$ Prandtl number	[-]
Q_{cd}	:	conduction heat flux	[W]
Q_{cv}	:	convection heat flux	[W]
Q_{loss}	:	heat loss	[W]

Q_{ncd}	:	$(= Q_{cd} - Q_{loss})$ net conduction heat flux	[W]
Q_{ncv}	:	$(= Q_{cv} - Q_{loss})$ net convection heat flux	[W]
r	:	position vector	[m]
R	:	$(= r/l)$ dimensionless position vector	[-]
Ra	:	$(=g\beta(\theta_h-\theta_c)l^3/(\alpha\nu))$ Rayleigh number	[-]
ds	:	tangential element of the coil	[m]
dS	:	$(= ds/l)$ dimensionless tangential element of the coil	[-]
t	:	Time	[s]
t_0	:	$(= l^2/\alpha)$ reference time	[s]
T	:	$(= (\theta-\theta_0)/(\theta_h-\theta_c))$ dimensionless temperature	[-]
u	:	velocity vector	[m/s]
u_0	:	$(= \alpha/l)$ reference velocity	[m/s]
U	:	$(= u/u_0)$ dimensionless velocity vector	[-]
Zc	:	Dimensionless distance between center of a cube and center of the coil (elevation)	[-]
α	:	thermal diffusivity	[m^2/s]
β	:	thermal expansion coefficient	[K^{-1}]

γ	:	$(=\chi_0 b_0^2/(\mu_m \rho g l))$ dimensionless gamma parameter indicating magnetic field strength	[-]
λ	:	thermal conductivity	[W/(m·K)]
ν	:	kinematic viscosity	[m²/s]
θ	:	Temperature	[K]
θ_0	:	(= 293 K) reference temperature	[K]
θ_c	:	temperature of cooled wall	[K]
θ_h	:	temperature of heated wall	[K]
ρ	:	density	[kg/m³]
ρ_0	:	reference density at temperature θ_0	[kg/m³]
τ	:	$(= t/t_0)$ dimensionless time	[-]
χ	:	mass magnetic susceptibility	[m³/kg]
χ_0	:	ref. volume magnetic susceptibility at θ_0	[-]
χ_m	:	$(=\chi \cdot \rho)$ volume magnetic susceptibility	[-]

Sub/Superscripts

0	:	reference value
c	:	cold
h	:	hot
cd	:	conduction
cv	:	convection

1 Introduction

Although the magnetic force has been known for many decades for ferromagnetic materials, the discovery of high-temperature superconductors in 1986 has opened the era on its study for general materials. With using a superconducting magnet many new phenomena have been reported in various fields of science. The super-computers gave an additional opportunity to solve numerically for complex problem prediction. Wakayama and coworkers have found both experimentally and numerically many notable magneto-aero dynamic phenomena which occur in a strong magnetic field. They work for example on promotion of combustion [1], breath supporting [2], magnetic levitation, jet stream of nitrogen gas into air [3] and so forth. Kitazawa's group have been also working on the phenomena associated with magnetic field. Among their many findings, they reported for example novel separation method for the feeble magnetic materials by the application of magneto-Archimedes levitation technique [4], enhancing oxygen gas dissolution into water [5], etc.

Bai *et al*. [6] developed a model equation for convection due to magnetic force and carried out numerical computations for jet flow of nitrogen gas in a decreasing gradient of magnetic field for, so to speak, a Wakayama jet. Huang *et al*. [7] carried out own mathematical model describing convection of paramagnetic and diamagnetic fluids and showed it together with the stability analysis. Tagawa *et al*. [8] derived the numerical model equations for magnetic

convection using a method similar to the Boussinesq approximation and carried out the numerical calculations. Kaneda *et al*. [9] studied the magnetic enhancement for the stably stratified air layer heated from above and cooled from below. The air was filled in a cubic enclosure located among the four poles magnet. The visualization with incense smoke showed that stagnant state was disturbed in the presence of magnetic field. The numerical analysis agreed well with the experiment to support governing equations. More information about magnetic convection and its applications can be found in book of Ozoe [10].

Krakov *et al*. [11,12] reported the study of magnetic field on the natural convection of magnetic fluid. They considered the system that the fluid is heated from below and cooled from above in a square or cubic enclosure. The effect of magnetic orientation [11] and the effect of magnetic strength [12] are studied. Their system is different from ours in various aspects as follows. They considered the artificial magnetic fluid with the base of kerosene which is different from ours such as air, water or present fluid (aqueous solution). They treated the 2D convection in a square cavity heated from below which is not stable in a gravity field. The 2D assumption for the flow presumes the same flow pattern in a horizontal direction of a long channel with a square cross section.

However, the theoretical work by S.H.Davis [13] and our experimental and numerical works [14,15] show that the roll cells are oriented with their axes horizontal and perpendicular to the long channel axis. These cells are no more 2D but 3D due to the rigid side walls on roll axes. Furthermore, the theory by S.H.Davis [13] suggests that the preferred orientation of roll cell is not deterministic in the cubic box heated from below. The numerical computation by Krakov *et al*. [12] also represents non-deterministic flow modes with upward flow at one corner and downward flow at three other corners, or vice versa. Due to these reasons, we will not compare the present work with those by Krakov *et al*. [11,12].

The present work concerns the magnetic convection of paramagnetic fluid in a cubic enclosure heated and cooled from side walls. This system was placed under the solenoid system of a superconducting magnet. The convection was investigated under several strengths of magnetic inductions to see their effect in the experiment as well as in the corresponding numerical computations.

2 Properties of the working fluid

The 80% mass aqueous glycerol solution was employed as a working fluid. This was mixed with crystals of gadolinium nitrate hexahydrate to make it paramagnetic. The thermophysical properties of the working fluid are listed in Table 1.

The density of the working fluid was measured with a pycnometer (*Brand 25ml*) and the viscosity with the Ostwald's viscometer. The thermal expansion coefficient was calculated from the measurements of the fluid density at different temperatures and the properties with

Table 1   Properties of the working fluid at the temperature of 298 K

Property	Value	Unit
α^*	1.01×10^{-7}	m^2/s
β	0.52×10^{-3}	K^{-1}
λ^*	0.397	W/(m·K)
μ	86.89×10^{-3}	Pa·s
ν	5.9×10^{-5}	m^2/s
ρ	1463	kg/m^3
χ	23.094×10^{-8}	m^3/kg
Pr	584	–

asterisk were estimated from [16]. The magnetic susceptibility was measured with the Magnetic Susceptibility Balance (MSB). Fig. 1 shows the mass magnetic susceptibility χ for various concentrations of gadolinium nitrate hexahydrate. The 80% mass concentration was employed for experiments.

3   Experimental system

Fig. 2 shows the experimental apparatus which was assembled from five separate elements. Those included two copper plates (one for cooling side, another one for heating side) with three holes in each to insert the thermocouples, the cubic cavity made of Plexiglas with the hole to fill the working fluid and the cooling and heating chambers made of Plexiglas. The cooling copper plate was cooled by the water flowing through the chamber pumped from a thermostating water bath while the heating copper plate was heated by the nichrome wire covered with a rubber and winded in the heating chamber. The internal size of the cavity was chosen to be 0.032 m.

The working fluid in the cubic enclosure was filled using a syringe and a thin needle. The front hole seen in
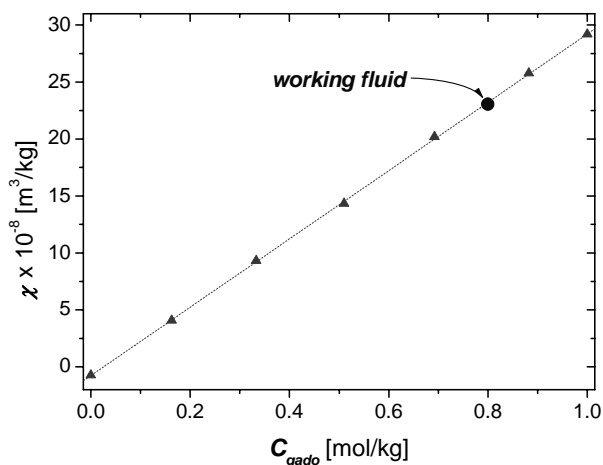

Fig. 1   Measured mass magnetic susceptibility plotted versus concentrations of Gd(NO$_3$)$_3$·6H$_2$O. The 80% mass glycerol aqueous solution was employed.
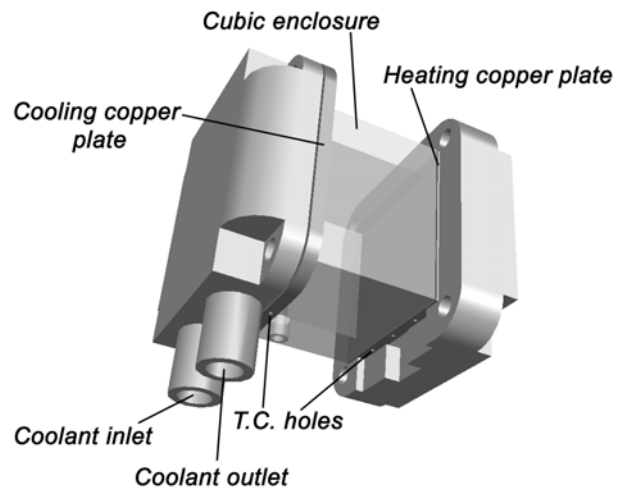

Fig. 2   Experimental apparatus

Fig. 2 was later closed by silicone resin to have no leakage of the fluid through it. The syringe was also very useful to remove unwanted air bubbles which appeared sometimes in the enclosure.

The experimental setup consisted of the experimental apparatus, the heater control system, the constant temperature bath and data acquisition system (*NEC3100*) connected to a personal computer. The temperature of the heated and cooled walls was measured by six T-type thermocouples. Two other thermocouples were used to monitor the temperature in the water bath and the room temperature. The current and voltage of heating power were regulated with two multimeters (*Keithley 2000*).

4   Experimental procedure

The heat transfer rates were measured with a 5 Tesla superconducting magnet, however the strength of magnetic force was not sufficient to carry out the visualization part. Therefore, visualization was done with a 10 Tesla superconducting magnet, with the enclosure placed just outside of the bore.

4.1   Heat transfer rates

The experimental apparatus was well insulated with cotton-wool and with vinyl foil. Then, the enclosure was placed in the bore of the 5 Tesla superconducting magnet in a distance of 0.07 m below from the solenoid center to ensure minimal radial component of the magnetic force whose value is proportional to ∇B^2. Fig. 3(b) right half shows that magnetic force vectors have almost uniform vertical direction in the cubical enclosure.

The heating power and the temperature of cooling water were set up. The temperatures of side walls were monitored, and when a steady state was reached, they were recorded. The steady state was attained usually in 2-3 hours. The magnetic field was applied to the system and the magnetic induction was changed from 0 T to 5 Tesla
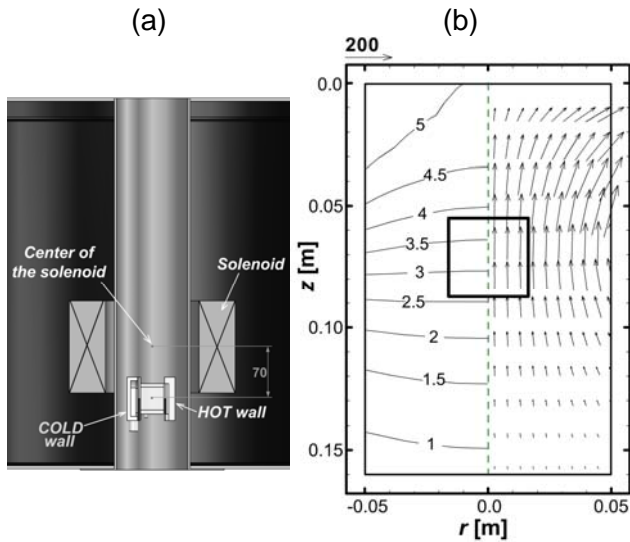
Fig. 3 (a) Location of the cube in the bore of the 5 Tesla superconducting magnet. (b) Magnetic field distribution (left half) with 5 T in the center of the solenoid system and vectors of ∇B^2 (right half) .Center of the solenoid is located at z=0.

step by step. After every step the system was kept to reach the steady state.

The Nusselt number is defined as follows:

$$Nu = \frac{Q_{ncv}}{Q_{ncd}} \quad (1)$$

In the present work, the method invented by Ozoe and Churchill [17] was used to estimate the net convection (Q_{ncv}) and net conduction heat fluxes (Q_{ncd}):

$$Q_{ncv} = Q_{cv} - Q_{loss} \quad (2)$$

$$Q_{ncd} = Q_{cd} - Q_{loss} \quad (3)$$

where Q_{cd} is the total heat supply during the conduction experiment and Q_{cv} the one during the convection experiment. Q_{loss} was assumed to depend only on the temperature of heated wall but not on the heat transfer mode inside the enclosure and was estimated from conduction experiment by the following equation:

$$Q_{loss} = Q_{cd} - A\lambda(\theta_h - \theta_c)/l \quad (4)$$

where $A\lambda(\theta_h - \theta_c)/l$ term represents the Fourier's law and $A = l^2$ is a conduction area of the cross-section. Heat loss (Q_{loss}) can be linearly approximated for various heating rates.

Having relations (2), (3) and (4), the equation (1) can be rewritten in the form:

$$Nu = \frac{Q_{cv} - Q_{loss}}{l\lambda(\theta_h - \theta_c)} \quad (5)$$

where the total heat supply is given by a product of current and voltage of the heater supply.

4.2 Visualization

The visualization of the temperature profiles was done with the 10 Tesla superconducting magnet. Very small amount of thermochromic liquid crystal slurry (*KWN-2025*) was added into the working fluid. Normally clean or slightly milky in appearance, the liquid crystals reflect definite colors at specific temperature and specific viewing angle. Therefore, the middle vertical cross-section of the cubic enclosure was illuminated by a white light generated by a halogen lamp. Thin slit film was placed at the film location of the projector so that slit light can be obtained for a long distance.

The red color is at 292.2 K red and blue color at 296.7 K. The experimental photographs were taken by a digital camera (EOS 10D + lens EF 70-200L) with an exposure time of 2 s.

Fig. 4 shows the photograph of the enclosure in the experiment under the bore of 10 Tesla superconducting magnet. The illuminating light was projected from above through the bore. The white light was reflected by the mirror placed above the magnet. Since the cubic enclosure was heated and cooled from side walls, the vertical mid-plane of the fluid was illuminated. The projector's focus was adjusted to keep sharp and thin light sheet coming through the cube's vertical cross-section. The camera was located away about 3 m from the magnet.
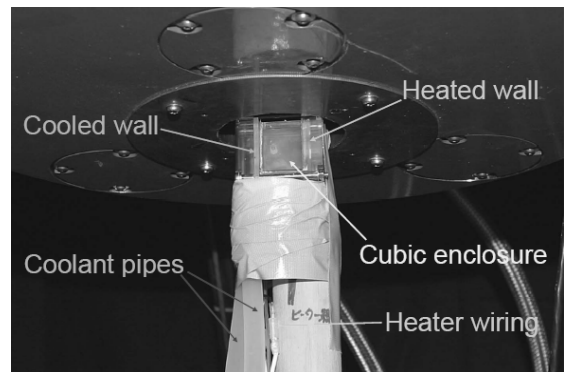

Fig. 4 Photograph of the enclosure position in the visualization part of the experiment

5 Numerical analysis

The numerical computations were based on the model for the magnetic convection of paramagnetic fluid derived by Bai *et al*. [6] and subsequently with Boussinesq approximation by Tagawa *et al*. [8]. It employs the fact, that the magnetic susceptibility of paramagnetic substance is inversely proportional to its absolute temperature (Curie's law). Therefore, if the temperature difference occurs in the paramagnetic fluid, the magnetic buoyancy force is generated in the presence of magnetic field. Some of our previous computations can be found in [18-20].

The governing equations in non-dimensional form are defined as follows:

$$\nabla \cdot U = 0 \tag{6}$$

$$\frac{DU}{D\tau} = -\nabla P + Pr\nabla^2 U + Ra\,Pr\,T\left[e_z - \gamma\frac{C}{2}\nabla B^2\right] \tag{7}$$

$$\frac{DT}{D\tau} = \nabla^2 T \tag{8}$$

Computational conditions are as follows:

$Pr = 100$; $C = 1+1/(\beta\theta_0)$; $Ra = 28040\cdot\Delta\theta$, $\gamma = 0.586 b_0^2$.

It should be mentioned that the flow and heat transfer characteristics are almost independent of the Pr number for higher Pr ($Pr > 10$) numbers fluids. Therefore inertia can be neglected and the Ra number is unique parameter to characterize the buoyant convection in the absence of magnetic field. That is why $Pr = 100$ was chosen in the numerical computations to get faster the final solution.

In order to compute the distribution of magnetic field, the Biot-Savart's law was used:

$$B = \frac{1}{4\pi}\oint_{multi-coil}\frac{dS \times R}{R^3} \tag{9}$$

The boundary conditions for this system are as follows:

$U = V = W = 0$	at all walls of the cube,
$T = 0.5$	at $X = -0.5$,
$T = -0.5$	at $X = 0.5$,
$\partial T/\partial Y = 0$	at $Y = -0.5, 0.5$,
$\partial T/\partial Z = 0$	at $Z = -0.5, 0.5$.

The initial condition is at a conduction state :

$U = V = W = 0$, $T = -X$ where $-0.5 \le X \le 0.5$.

The average Nusselt number was computed on the hot wall from the following definition:

$$Nu = \frac{\int_{-0.5}^{0.5}\int_{-0.5}^{0.5}(\partial T / \partial X)_{X=-0.5}^{cv}dYdZ}{\int_{-0.5}^{0.5}\int_{-0.5}^{0.5}(\partial T / \partial X)_{X=-0.5}^{cd}dYdZ} \tag{10}$$

The above equations were approximated with the finite difference equations. The HSMAC method was used to iterate mutually the pressure and velocity field and the number of meshes was chosen to be 40x40x40. The grid dependency test for the same model equations was carried out in our previous work [19] and has showed that the effect of grid size was slight comparing with the mesh 30x30x30.

6 Results

The numerical computations were carried out for the dimensionless conditions of the experiments. At first heat transfer rates are compared with those obtained for 5 Tesla superconducting magnet and then the visualization experiment with the 10 Tesla magnet .

6.1 Heat transfer rates

The Nusselt number was estimated from equation (5). Fig. 5 shows corresponding, vertical cross-section of the modeled system for the numerical computations. Axial dimension in this figure is non-dimensionalized.

Fig. 5 shows also the forces acting on the fluid. The arrow symbols indicate the relative force balance in
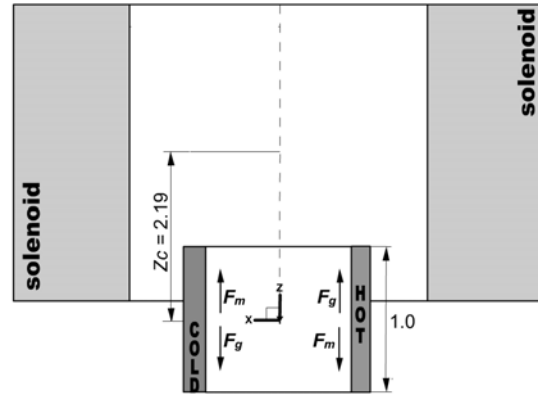

Fig. 5 Schematic view of the cross-section of the system with 5 Tesla magnet for the comparison of Nu numbers

terms of those at the average temperature. The gravity force is always working downwards but net flow becomes upward for hot fluid and downwards for cold fluid in terms of the average temperature fluid. It is the same for the magnetic force. Thus, for this configuration, the magnetic buoyancy force F_m acts in the opposite direction against the gravitational buoyancy force F_g. Near the heated wall (on the right-hand side), F_m acts downward while near the cooled wall (left-hand side) upward. The gravitational buoyancy force acts in the opposite direction as seen in Fig. 5.

Table 2 gathers experimental conditions and their corresponding non-dimensional parameters for heat transfer experiment with 5 Tesla super-conducting magnet.

Fig. 6 shows the comparison between experimental and numerical results. The Nusselt numbers are plotted versus the maximum induction. As shown in Fig. 5, the magnetic and gravitational buoyancy forces act in the

Table 2 Experimental data and its non-dimensional values for heat transfer experiment with 5 Tesla super-conducting magnet

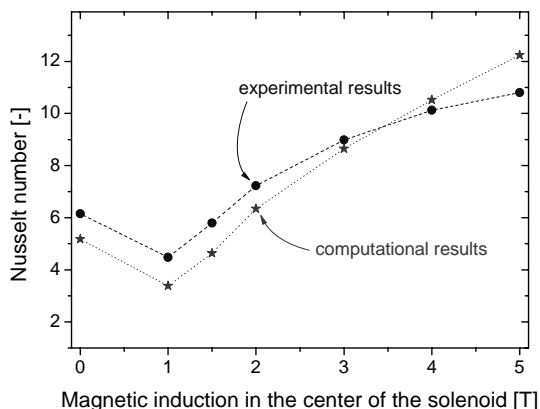| b_0 [T]	γ [−]	Temp. hot	Temp. cold	Temp. difference	Rayleigh number
0	0	22.54	17.67	4.87	1.38×10^5
1	0.59	23.56	17.79	5.77	1.62×10^5
2	2.34	22.13	17.71	4.42	1.24×10^5
3	5.27	21.60	17.75	3.85	1.08×10^5
4	9.37	21.31	17.76	3.55	0.99×10^5
5	14.64	21.13	17.74	3.39	0.95×10^5

Fig. 6 Comparison of the Nusselt numbers at $Ra_0 = 1.38 \times 10^5$. (See Table 2 for details.)

opposite direction and when the strength of magnetic field is weak, they are compensating each other. The Nusselt number have its minimum around $b_{max} = 1$ Tesla, both in the numerical and experimental analyses. For larger b_{max}, the Nusselt number increases with increasing magnetic induction. Therefore, it can be said that when the magnetic field strength increases, the magnetic buoyancy force becomes dominant and the convection is enhanced.

6.2 Visualization

In the visualization part, the 10 Tesla superconducting magnet was used. The enclosure could be then placed just outside of the bore of the magnet to make the visualization procedure possible. Fig. 7 shows the corresponding cross-section view of the system for the numerical computations.

Table 3 gathers experimental conditions and their corresponding non-dimensional parameters for visualiza-
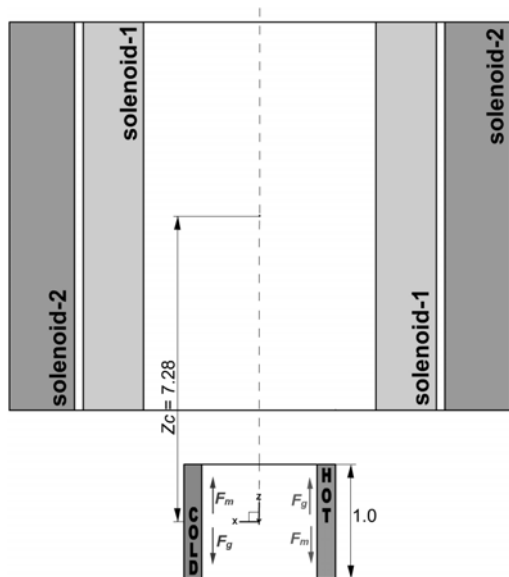

Fig. 7 Schematic view of the cross-section of the system with the 10 Tesla magnet for the comparison of temperature distributions.

Table 3 Experimental data and its non-dimensional parameters for visualization experiment with 0 Tesla super-conducting magnet

b_0 [T]	γ [−]	Temp. hot	Temp. cold	Temp. difference	Rayleigh number
0	0	20.81	17.90	2.91	8.16×10^4
5	14.64	21.14	17.96	3.18	8.92×10^4
6	21.09	21.21	17.96	3.25	9.11×10^4
8	37.49	20.54	17.96	2.58	7.23×10^4

tion experiment with 10 Tesla super-conducting magnet.

Fig. 8 shows numerical results in the form of resultant force vectors and longtime streak lines for four cases which correspond to the experiment at 0, 5, 6 and 8 Tesla of the magnetic induction respectively. Fig. 9 shows the corresponding vertical cross-section of the temperature field. In Fig. 9, the left-hand side column shows the experimental results with the isolines obtained with PIT (Particle Image Thermometry) method [21] and the right-hand side column shows temperature distributions computed numerically.

At 0 Tesla the usual gravitational convection occurred. The force vectors near the hot part of the enclosure direct upward, while the force vectors near the cold part of the cube direct downward. When the magnetic field is imposed, the magnetic buoyancy force is expected to cancel or overcome the gravity effect.

When the magnetic induction is 6 Tesla, the numerical computation shows two rolls in a vertical cross-section (Fig.8 c). At this case, the balance between gravitational buoyancy force and magnetic buoyancy force is attained. Fig. 9 shows corresponding isotherms. In the experiment the upper and lower rolls were not in the same size since even small difference in the magnetic strength affected the final profile of steady state. At 8 Tesla, the magnetic force becomes dominant, and the convection is reversed in comparison to that at 0 Tesla.

Comparison between experimental and numerical isotherms shows good agreement and proves the correctness of the applied numerical model.

7 Conclusions

The heat transfer rates of magnetic convections in a cubic enclosure placed below the magnet coil were measured with 5 Tesla magnet for 80% mass concentration of aqueous glycerol solution with 0.8 mol/kg of gadolinium nitrate hexahydrate. The isothermal profiles were also pictured with liquid crystal slurry dispersed in the fluid. The visualization experiments were carried out with 10 Tesla superconducting magnet. These results were employed to compare with the numerical computations for the almost same conditions. Both the average Nusselt numbers and the isothermal profiles represented good correspondence to each other to assure the model equations and the numerical approach.
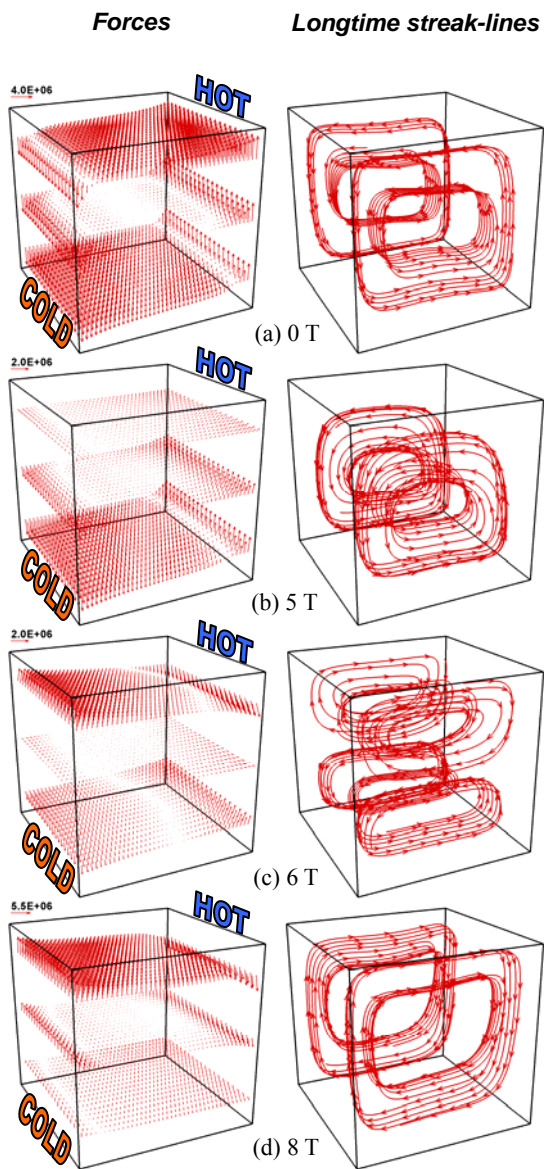
　　　　© 2006 *The Heat Transfer Society of Japan*

Forces　　**Longtime streak-lines**

(a) 0 T

(b) 5 T

(c) 6 T

(d) 8 T

Fig. 8　Numerical results computed at four different strengths of magnetic induction. Left column: force vectors, right: longtime streak lines

Temperature distributions:
experiment　　**computations**

(a)　0 T
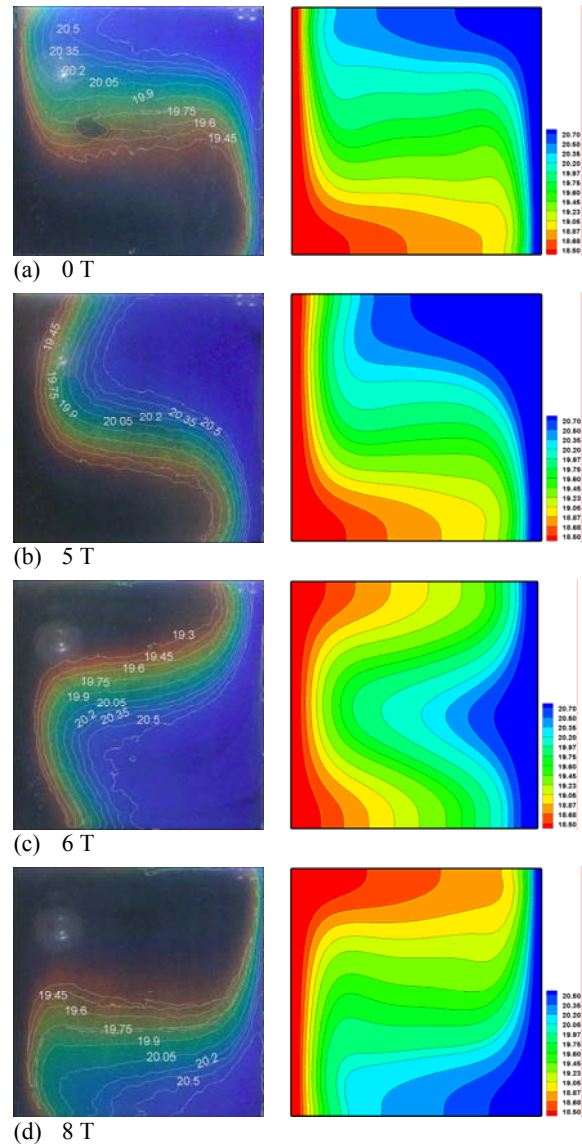
(b)　5 T

(c)　6 T

(d)　8 T

Fig. 9　Comparison of the isotherms obtained in the experiment and the numerical computations at four different strengths of magnetic induction

Acknowledgments

References

[1]　Wakayama, N. I., "Magnetic promotion of combustion in diffusion flames", *Combustion and Flame*, 93 (1993), 207-214.

[2]　Wakayama, M., and Wakayama, N. I., "Magnetic acceleration of inhaled and exhaled flows in breathing", *Japanese J. Applied Physics*, 39 (2000), 262-264.

[3]　Wakayama, N. I., "Effect of decreasing magnetic field on the flow of nitrogen gas", *Chem. Phys. Letters*, 185 (1991), 449-451.

[4]　Hirota, N., Ikezoe, Y., Uetake, H., Kaihatsu, T., Takayama, T., and Kitazawa, K., "Magneto-Archimedes levitation and its application", *RIKEN Rev.*, 44 (2002), 159-161.

[5]　Ikezoe, Y., Hirota, N., Sakihama, T., Mogi, K., Uetake, H., Homma, T., Nakagawa, J., Sugawara, H., and Kitazawa, K., "Acceleration effect of the rate of dissolution of oxygen in a magnetic field", *J. of Jap. Inst. of Applied Magnetics*, 22 (1998), 821-824.

[6] Bai, B., Yabe, A., Qi, J.W., Wakayama N.I., Quantitative analysis of air convection caused by magnetic-fluid coupling, *AIAA Journal*, 37:12 (1999), 1538-1543.

[7] Huang, J., Gray, D.D., and Edwards, B.F., "Thermoconvective instability of paramagnetic fluids in a nonuniform magnetic field", *Phys. Rev. E*, 57 (1998), 5564-5571.

[8] Tagawa, T., Shigemitsu, R., and Ozoe, H., "Magnetizing force modeled and numerically solved for natural convection of air in a cubic enclosure: effect of the direction of the magnetic field", *Int.J.Heat Mass Transfer*, 45 (2002), 267-277.

[9] Kaneda, M., Tagawa, T., and Ozoe, H., "Convection induced by cusp-shaped magnetic field for air in a cube heated from above and cooled from below", *J. Heat Transfer*, 124 (2002), 17-25.

[10] Ozoe, H., "Magnetic Convection", Imperial College Press, ISBN 1-86094-578-3 (2005).

[11] Krakov, M.S., Nikiforov, I.V., "To the influence of uniform magnetic field on thermomagnetic convection in square cavity, *Journal of Magnetism and Magetic Materials, 252(2002)*209-211.

[12] Krakov, M.S., Nikiforov, I.V., Reks, A.G., "Influence of the uniform magnetic field on natural convection in cubic enclosure: experiment and numerical simulation", *Journal of Magnetism and Magnetic Materials*, 289 (2005), 272-274.

[13] Davis, S.H., "Convection in a box: linear theory", *J. Fluid Mechanics*, 30 (1967), 465-478.

[14] Ozoe, H., Sayama, H., Churchill, S.W., "Natural convection in an inclined square channel", *Int. J. Heat Mass Transfer*, 17 (1974), 401-406.

[15] Ozoe, H., Yamamoto, K., Sayama, H., Churchill, S.W., "Natural circulation in an inclined rectangular channel heated on one side and cooled on the opposing side," *Int. J. Heat Mass Transfer*, 17 (1974), 1209-1217.

[16] Lide, D.R., "Handbook of Chemistry and Physics", Chemical Rubber Company Press, Baca Raton, FL, 2001-2002.

[17] Ozoe, H., Churchill, S.W., "Hydrodynamic stability and natural convection in Newtonian and non-Newtonian fluids heated from below", *AIChE Symposium Series Heat Transfer*, 69 (1973), 126-133.

[18] Bednarz, T., Tagawa, T., Kaneda, M., Ozoe, H., Szmyd, J.S., "Magnetic and gravitational convection of air with a coil inclined around the X axis", *Numerical Heat Transfer*, 46 (2004), 99-113.

[19] Bednarz, T., Tagawa, T., Kaneda, M., Ozoe, H., Szmyd, J.S., "Convection of air in a cubic enclosure with an electric coil inclined in general orientations", *Fluid Dynamics Research*, 36 (2005), 91-106.

[20] Bednarz, T., Tagawa, T., Kaneda, M., Ozoe, H., Szmyd, J.S., "Numerical study of joint magnetisation and gravitational convection of air in a cubic enclosure with an inclined electric coil," *Progress in Computational Fluid Dynamics*, 5 (2005), No. 3/4/5.

[21] Kowalewski, T., "Experimental methods for quantitative analysis of thermally driven flow, experimental benchmarks for code validations", 5 lectures from Advanced School on Phase Change with Convection – modeling and validation: Coordinated by Prof. Kowalewski and Prof. Gobin, CISM, Udine, Italy, 2002.